Effects of Interaction of Photosensitizer with DNA and Stacked G Bases on Photosensitized One-Electron Oxidation of DNA

Tadao Takada, Kiyohiko Kawai, Sachiko Tojo, and Tetsuro Majima*

The Institute of Scientific and Industrial Research (SANKEN), Osaka University, Mihogaoka 8-1, Ibaraki, Osaka 567-0047, Japan

Received: March 11, 2003; In Final Form: October 7, 2003

Three naphthalimide (NI) derivatives (NIN, NIP, and NIO) as photosensitizers for the G-selective oxidation were synthesized, and the mechanism of the photosensitized one-electron oxidation of DNA by the NI derivatives was studied. NIN possessing a cationic side chain exhibited strong association with the oligodeoxynucleotides (ODNs) due to an electrostatic interaction between the phosphate groups of ODN and the cationic group of NIN, while no association was observed for NIP possessing an anionic side chain due to electrostatic repulsion among the phosphate groups. The DNA-binding properties of NIO with a neutral side chain were intermediate between those of NIN and NIP. The effects of the electrostatic interaction and repulsion between the NI derivatives and ODN and stacked G bases on the photosensitized one-electron oxidation of ODN were studied by the nanosecond transient absorption measurement and HPLC analysis. The yield of the NI derivatives in the triplet excited state (^{3}NI*) observed immediately after a 355-nm laser flash decreased with an increase in the binding constants, and almost no transient absorption was observed when NIN was used as a photosensitizer. This result indicates that rapid charge separation occurs between the NI in the singlet excited state (^{1}NI*) and the adjacent nucleobase, followed by a rapid charge recombination between the NI radical anion and the adjacent nucleobase radical cation when NIN is bound to ODN. Therefore, the sequence dependence of the one-electron oxidation of ODN was investigated using NIP, which does not bind to ODN. By monitoring the one-electron reduced form of NIP ($NIP^{\bullet-}$) produced by the electron transfer from ODN to ^{3}NIP*, we found that the charge-separation efficiency increased with the sequence of sequential G's, such as GG and GGG, because of the oxidation potential of G decreased by the stacking effect of G's. To clarify the relationship between the formation of the transient intermediates observed during the LFP and actual amount of ODN oxidative damage, we performed the quantitative analysis of the ODN oxidative lesion caused by the NI derivatives using HPLC. With respect to the sequence of ODN, larger amounts of G consumed by the photosensitized one-electron oxidation were observed with ODN possessing multiple G, GG, and GGG compared to a single G. In contrast to the LFP experiments, a similar amount of oxidative damage was observed for three synthetic NI derivatives, indicating that the association of the NI derivatives to ODN apparently has no effect on the one-electron oxidative process. This might be due to the O_2 involved in the one-electron oxidation process. These results are discussed in the context of the concentration of O_2 in the solution.

Introduction

It is possible to utilize a molecule capable of delivering the chemical activity on demand with external stimuli as a probe for cellular processes, and many compounds possessing such functions have been synthesized and investigated.[1] Photochemical control of the chemical activity has been used to induce DNA lesions leading to tumor destruction and applied to photodynamic therapy (PDT). The photochemical mechanism of the DNA lesion is divided into three parts: generation of singlet oxygen and hydroxyl radical, hydrogen abstraction from the sugar unit, and redox reaction.[1]

There has been a great interest in the one-electron oxidation of DNA in connection with DNA damage caused by ionizing radiation, oxidizing agents, and photoirradiation with photosensitizers.[1,2] The one-electron oxidation of DNA leading to a base lesion occurs at guanine (G), which is the primary target in DNA because it has the lowest oxidation potential among the four nucelobases.[3,4] Furthermore, it is known that the oxidative lesion of G selectively occurs at consecutive G's, GG and GGG, compared to the single G.[5] This characteristic of the oxidation of DNA can be used for site-selective DNA cleavage leading to tumor destruction.

Properties of the excited states, reactive species, and intermediates on the photochemical oxidation responsible for DNA damage should be first considered to understand the photochemical mechanism and to obtain valuable information for the molecular design of photosensitizer.[6−9] The oxidative damage site along the DNA strand has been extensively investigated at the base sequence level using high-resolution polyacrylamide gel electrophoresis (PAGE).[2] On the other hand, only a few studies have been reported about the one-electron oxidation of DNA using transient absorption measurements.[6,8,10,11] It is important to elucidate the mechanism of DNA oxidation in connection with the migration of a hole generated in DNA.[12] In the present study, we have synthesized three naphthalimide

* Corresponding author. Tel: +81-6-6879-8495. Fax: +81-6-6879-8499. E-mail: majima@sanken.osaka-u.ac.jp.

10.1021/jp034612s CCC: $27.50
Published on Web 12/17/2003

SCHEME 1: Structure of Naphathalimide (NI) Derivatives and Sequences of Synthetic Oligodeoxynucleotides (ODNs) Used in This Study

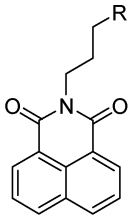

R: -NMe_2H^+ (NIN)
-OH (NIO)
-OPO_3H^- (NIP)

5'-TGTGTGTGTGTGT-3'
3'-ACACACACACACA-5' ODN-G1

5'-TTGGTTGGTTGGT-3'
3'-AACCAACCAACCA-5' ODN-G2

5'-TTGGGTTTGGGTT-3'
3'-AACCCAAACCCAA-5' ODN-G3

SCHEME 2: Mechanism of NI-Photosensitized One-Electron Oxidation of ODN Involving NI in the Singlet and Triplet Excited States (^{1}NI* and ^{3}NI*, Respectively), Giving NI Radical Anion ($NI^{\bullet-}$) and G Radical Cation ($G^{\bullet+}$) in ODN[a]

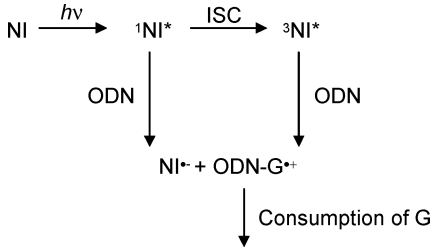

[a] ISC denotes intersystem crossing.

(NI) derivatives as the photosensitizer for the G-selective oxidation to examine the effects of the interaction toward oligodeoxynucleotides (ODNs) for the one-electron oxidation of DNA (Scheme 1). The high efficiency of the intersystem crossing of NI and large extinction coefficients of NI in the triplet state and NI reduced form are advantageous for the detection of these transient intermediates during the laser flash photolysis. NI possessing a cationic side chain (NIN) exhibited a strong association due to the electrostatic interaction between the phosphate groups of ODN and the cationic group, while no association was observed for NI derivatives possessing a phosphate group (NIP) because of electrostatic repulsion among the phosphate groups. These NI derivatives are expected to have almost the same redox properties except for the binding properties because their substituent groups were linked to the NI chromophore by an $n = 3$ methylene linker (Scheme 1). The photochemical mechanism of the one-electron oxidation of ODN by three NI derivatives was studied using laser flash photolysis (LFP) experiments.[9,13,14] The effects of the interaction between the photosensitizer and ODN and ODN sequence on the one-electron oxidation of ODN were examined by monitoring NI in the excited state and reduced form (Schemes 1 and 2). Besides, to clarify the relationship between the formation of the transient intermediates observed during the LFP and actual amount of ODN oxidative damage, we performed the quantitative analysis of the ODN oxidative lesion by the synthetic photosensitizer using HPLC and discuss the importance of the O_2 concentration in the solution.

Experimental Section

Materials. *Oligodeoxynucleotides (ODNs).* The ODNs were synthesized using an Applied Biosystems DNA synthesizer with standard solid-phase techniques and purified on a JASCO HPLC using a reverse-phase C-18 column with an acetonitrile/50 mM ammonium formate gradient. Duplex solutions (20 mM sodium phosphate buffer, pH 7) were prepared by mixing equimolar amounts of the desired ODN complements and annealing with gradual cooling from 80 °C to room temperature.

*N-(3-Hydroxypropyl)-1,8-naphthalimide (**1**).* **1** was synthesized according to the previous report.[13]

N-[3-(Dimethylamino)propyl]-1,8-naphthalimide (**2**). *N,N*-Dimethyl-1,3-propanediamine (5.7 mL, 54 mmol) was added dropwise over 30 min to a solution of 1,8-naphthalic anhydride in 23 mL of *N,N*-dimethylacetamide. The reaction mixture was heated at 100 °C for 1.5 h. The crude mixture was concentrated on a rotary evaporator, and the residue was subjected to silica gel column chromatography (ethyl acetate/methanol) (3.9 g, 90%). ^{1}H NMR (DMSO-d_6) δ 1.74 (m, 2H, $-CH_2$), 2.12 (s, 6H, $-CH_3$), 2.29 (t, 2H, $-CH_2$), 4.06 (t, 2H, $-CH_2$), 7.86 (t, 2H, napht), 8.46 (d + d, 4H, napht). FAB MASS (positive ion): *m/e* 283 (M + H).

N-[3-(Dimethylamino)propyl]-1,8-naphthalimide Hydrochloride. Solution of 1 N HCl−ether was added to a solution of *N*-[3-(dimethylamino)propyl]-1,8-naphthalimide (1.0 g, 3.5 mmol) dissolved in 20 mL of methanol. After being stirred for 2 h under an atmosphere of N_2, the solution was diluted with 100 mL of ether. The precipitates were filtered and washed with ether to give the desired products as a white powder (0.9 g, 80%). ^{1}H NMR (D_2O) δ 1.90 (m, 2H, $-CH_2$), 2.72 (s, 6H, $-CH_3$), 3.03 (t, 2H, $-CH_2$), 3.80 (t, 2H, $-CH_2$), 7.40 (2H, t, napht), 7.92 (4H, d + d, 4H, napht). ^{1}H NMR (DMSO-d_6) δ 2.06 (m, 2H, $-CH_2$), 2.73 (s, 6H, $-CH_3$), 3.14 (t, 2H, $-CH_2$), 4.13 (t, 2H, $-CH_2$), 7.90 (2H, t, napht), 8.51 (4H, d + d, napht). FAB MASS (positive ion): *m/e* 283 (M − Cl).

N-(Propyl)-1,8-naphthalimide, 3′-Dimethyl Phosphate Ester. Phosphorylation of **1** was carried out according to the procedure reported previously.[15] *N*-(3-Hydroxypropyl)-1,8-naphthalimide (1.0 g, 3.9 mmol) and carbon tetrabromide (1.43 g, 4.3 mmol) were dissolved in 2.0 mL of pyridine under N_2 atmosphere. The resulting solution was cooled to 0 °C with an ice-cold bath, and then trimethyl phosphite (0.59 mL, 4.9 mL) was added to it in a dropwise manner. After completion of addition of trimethyl phosphite, the ice bath was removed, and the reaction mixture was allowed to stir at room temperature. After being stirred for 2.5 h, the reaction mixture diluted with 20 mL of ether was transferred into a separatory funnel and then washed with 5% HCl (2 × 6 mL), saturated aqueous $NaHCO_3$ (1 × 6 mL), and brine (1 × 6 mL). The organic layer was dried over anhydrous Na_2SO_4 and concentrated under reduced pressure. The residue was purified by silica gel chromatography to give 0.68 g of the desired product as a white solid (48%). ^{1}H NMR (DMSO-d_6) δ 2.02 (m, 2H, $-CH_2$), 3.65 (d, 6H, $-CH_3$), 4.09 (q, 2H, $-CH_2$), 4.16 (t, 2H, $-CH_2$), 7.88 (t, 2H, napht), 8.49 (d + d, 4H, napht). FAB MASS (positive ion): *m/e* 364 (M + H).

N-(Propyl)-1,8-naphthalimide, 3′-Phosphoric Acid. Chlorotrimethylsilane (0.53 mL) was added dropwise to a mixture of **1** (630 mg, 1.7 mmol) and NaI (623 mg, 4.2 mmol) dissolved in dry CH_3CN (2 mL). After being stirred for 2 h in the dark, the reaction mixture was centrifuged, and the precipitated sodium chloride was washed with CH_2Cl_2 (3 × 1 mL). After evaporation of combined supernatants, the residue was dissolved in CH_2Cl_2 (10 mL) and extracted with water (3 × 30 mL). The aqueous layer concentrated under reduced pressure was purified by HPLC on a reverse-phase C-18 column with an acetonitrile/50 mM ammonium formate gradient. ^{1}H NMR (DMSO-d_6) δ 1.96 (m, 2H, $-CH_2$), 3.93 (q, 2H, $-CH_2$), 4.13 (t, 2H, $-CH_2$),

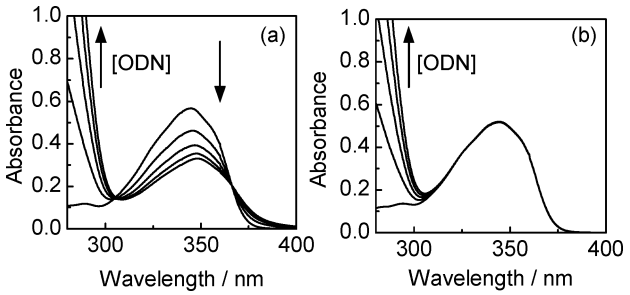

Figure 1. Ground-state absorption spectral changes observed upon addition of ODN-G1 (0, 7.3, 14, 21, and 27 μM, strand concn) to 40 μM NIN (a) and 40 μM NIP (b) in 20 mM sodium phosphate buffer (pH = 7.0).

7.88 (t, 2H, napht), 8.49 (d + d, 4H, napht). FAB MASS (positive ion): *m*/*e* 336 (M + H).

General Technique. The ground-state UV/vis absorption spectra were measured using a JASCO V-530 double-beam spectrophotometer. The proton NMR spectra were recorded on a JEOL 270 MHz NMR spectrometer. The HPLC analysis was carried out using a JASCO PU-1580 HPLC system equipped with a Cosmosil 5C18-MS column (4.6 mm × 150 mm). Detection was carried out by monitoring the absorbance at 254 nm. Silica gel column chromatography was carried out on Wakogel C-200, and thin-layer chromatography was on a Merck silica gel $60F_{254}$ plate. The nanosecond transient absorption measurement was performed using the LFP technique.[10] The third-harmonic oscillation (355 nm, 4 ns, 15 mJ) from a Q-switched Nd:YAG laser (Quantel model Brilliant) was used for the excitation light. A xenon flash lamp (Osram, XBO-450) was focused into the sample solution as the probe light for the transient absorption measurement. Time profiles of the transient absorption in the UV−visible region were measured with a monochromator (Nikon G250) equipped with a photomultiplier (Hamamatsu Photonics R928) and digital oscilloscope (Tektronics, TDS-380P).

HPLC Analysis. Irradiation of each reaction mixture containing ODN (40 μM strand concentrated) and the NI derivatives (40 μM) in pH 7.0 sodium cacodylate buffer (20 mM) was carried out using a high-pressure Hg lamp fitted with a 330 nm cutoff filter for 10 min. The reaction mixture was directly subjected to enzymatic digestion with snake venom P. D. E., P1 nuclease, and alkaline phosphatase. The consumption of G was quantified by reverse-phase HPLC.

Results and Discussion

Interaction between NI Derivatives and Oligodeoxynucleotides (ODNs). To examine the effects of the charge of side chains in three synthetic NI derivatives on the binding to the oligodeoxynucleotides (ODNs) shown in Scheme 1, we observed the ground-state absorption spectral changes of each NI derivative upon the addition of each ODN.[6] As shown in Figure 1, the ground-state absorption spectra of NIN possessing a cationic side chain changed upon the addition of ODN and exhibited a bathochromic shift relative to that of the free NIN (Figure 1a). On the other hand, the anionic NIP showed no change in the absorption spectrum, indicating no association of NIP with ODN (Figure 1b). The binding constants (*K*) of the NI derivatives to ODN (eq 1) were determined by fitting the change of absorption

$$\mathrm{ODN} + \mathrm{NI} \rightleftharpoons \mathrm{ODN/NI} \qquad (1)$$

to the McGhee and von Hippel equation[16] and are shown in Table 1.

TABLE 1: Binding Constants (*K*) of NI Derivatives to ODN-G1, -G2, and -G3

NI derivative	ODN	K (10^4 M^{-1})
NIN	G1	4.7
	G2	2.8
	G3	2.1
NIO	G1	0.6
	G2	<0.6
	G3	<0.6
NIP		~0

SCHEME 3: Schematic Illustration of Interaction between NI Derivatives and ODN

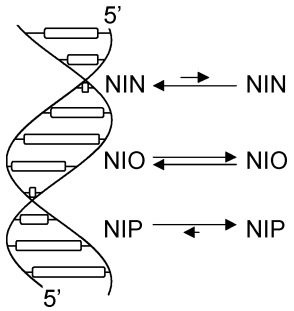

The *K* values of the NI derivatives to G1 are in the order NIP < NIO < NIN. This result shows that the association of each NI derivative to ODN is dependent upon the charge of the side chain. Because *K* of NIN is the largest among the NI derivatives, it is indicated that NIN, possessing the positive charge, strongly binds to the ODN phosphate moiety by an electrostatic interaction (Scheme 3). Besides, statistical distributions of both NIN and NIO along ODN were almost equivalent because the UV spectral changes upon the addition of ODN to the solution of the NIN and NIO derivatives were almost the same. On the other hand, no interaction of the anionic NIP was observed because of repulsion of the negatively charged NIP versus the negatively charged ODN backbone. When NI derivatives interact with ODN, NI can intercalate between two nucleobases of ODN because of the planar structure of the naphthalene unit.[6,17] With respect to the sequence-dependent interaction between NIN and ODN, *K* decreased in the order G1 > G2 > G3 (Table 1), indicating that the stacking of GG and GGG induced rigidity to the ODN structure, which is unfavorable for NIN intercalation.[18]

NI Derivatives in the Excited State. Photophysical studies of the NI derivatives in the excited state and photoreaction of the NI derivatives with ODN have been previously reported.[14] The transient properties of 1,8-naphthalimide derivatives have already been studied, and the triplet−triplet absorption and transient absorption of the radical anion of the 1,8-naphthalimide derivatives have been measured by LFP.[6,13] As shown in Figure 2, the transient absorption spectral changes were observed during the LFP of NIP with the 355-nm laser excitation. Immediately after a 355-nm laser flash, a transient absorption spectrum with a peak at 475 nm was observed and assigned to NIP in the triplet excited state (^{3}NIP*). This transient absorption of ^{3}NIP* decayed with an increase in a new peak at 400 nm assigned to the NIP radical anion ($NIP^{\bullet -}$). This decay rate of ^{3}NIP* was dependent upon the concentration of NIP. Therefore, it is suggested that ^{3}NIP* decayed through the self-quenching process to give $NIP^{\bullet -}$ and the NIP radical cation ($NIP^{\bullet +}$) as reported previously.[6] Because the extinction coefficient of the absorption peak of $NIP^{\bullet +}$ is much smaller than that of $NIP^{\bullet -}$, the absorption of only $NIP^{\bullet -}$ was observed concomitant with

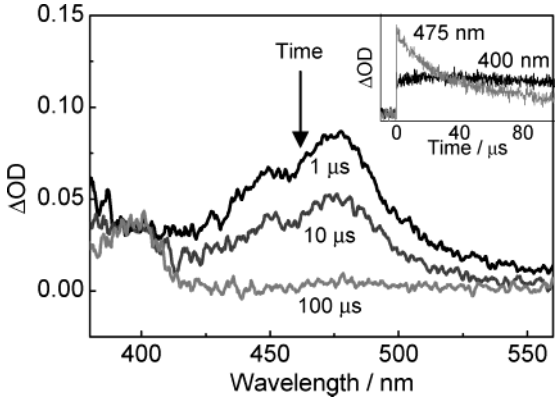

Figure 2. Transient absorption spectra observed at 1, 10, and 100 μs after the 355-nm laser flash during the LFP of 40 μM NIP in 20 mM sodium phosphate buffer (pH = 7.0) under argon-saturated conditions. Inset shows the time profiles measured at 400 and 475 nm.

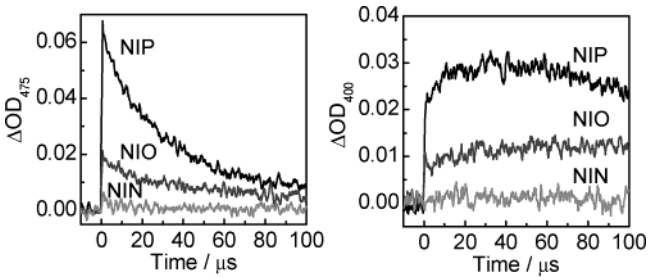

Figure 3. Time profiles of transient absorption of ^{3}NI* derivatives observed at 475 nm (a) and NI$^{\bullet-}$ at 400 nm (b) in the presence of ODN-G1 after the laser flash (λ_{ex} = 355 nm). Concentration of NI derivatives and ODN-G1 were 40 μM and 100 μM (strand concn), respectively.

the decay of ^{3}NIP*. Other NI derivatives, NIN and NIO, showed a similar behavior, while the decay rates of ^{3}NI* were different.

The one-electron reduction potentials of the NI derivatives were previously determined by cyclic voltammetry to be −0.84 V vs NHE.[6,13] On the basis of the reduction potential and zero−zero excitation energy of the triplet state, the reduction potential of ^{3}NI* was estimated to be 1.5 V. Considering that the one-electron oxidation potentials of nucleobases are 1.29 (G), 1.42 (A), 1.6 (C), and 1.7 (T) (V vs NHE at pH 7),[3] it is expected that ^{3}NI* selectively oxidizes G compared with other nucleobases as previously reported.[13] Namely, using ^{3}NI* as an oxidant, we can examine the one-electron oxidation process of G in ODN.

Effects of Interaction between NI Derivatives and ODN on the One-Electron Oxidation. To elucidate the effects of the interaction between NI derivatives and ODN on the one-electron oxidation of ODN, we examined the LFP of a mixture of ODN and NI derivatives. The transient absorption spectral changes were observed during the LFP, similar to those for the NI derivatives in the absence of ODN. However, in the case of NIP, the absorption at 400 nm assigned to NIP$^{\bullet-}$ increased in the presence of ODN because of the electron-transfer quenching of NI in the triplet state by ODN. Time profiles of the transient absorption with a peak at 475 nm, assigned to the NI derivatives in the triplet excited state (^{3}NI*), were observed during the 355-nm LFP in the presence of ODN-G1 as shown in Figure 3. The transient absorption of NI$^{\bullet-}$ monitored at 400 nm overlapped with that of NI in the triplet state. The charge-separation yield was too low to analyze the kinetics of formation of NI$^{\bullet-}$ in detail. The yield of ^{3}NI* obtained immediately after the 355-nm laser flash excitation decreased with an increase in the *K* of the NI derivatives to ODN. No ^{3}NIN* formed during the LFP of NIN in the presence of ODN, while ^{3}NIP* formed in a yield nearly identical to that in the absence of ODN. NIN in the ground state strongly associates with ODN, while NIP in the ground state does not associate with ODN. These results indicate that the rapid charge separation between NI in the singlet excited state (^{1}NI*) associated with ODN and adjacent nucleobase occurs within a laser flash (4 ns),[6] followed by rapid charge recombination between NI$^{\bullet-}$ and the adjacent nucleobase radical cation. Therefore, the formation of NIO and NIN in the triplet excited state (^{3}NIO* and ^{3}NIN*) was suppressed. The photosensitizer in the excited state associated with ODN is efficiently quenched via rapid charge separation and recombination, which prevent reactions of the nucleobase radical cation, especially G$^{\bullet+}$, with H_2O and O_2 leading to decomposition. Subsequently, the effective oxidation of ODN is unlikely to occur. In other words, the photosensitized one-electron oxidation of ODN occurs more effectively with the nonassociated ("free") NI (NIP) compared with the associated NI (NIN and NIO). Therefore, the results from the LFP measurements demonstrated that the formation of ^{3}NI* is important for the effective photooxidation of ODN responsible for the oxidative lesion.

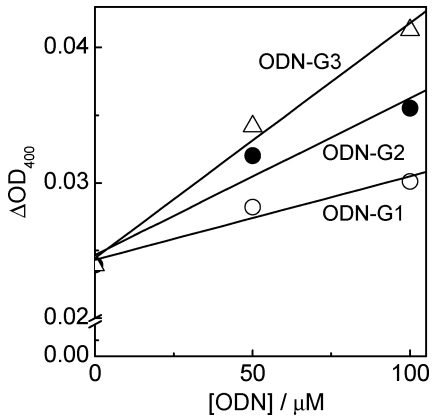

Figure 4. Plots of ΔOD_{400}, indicating the concentration of NIP$^{\bullet-}$, observed after the laser flash (λ_{ex} = 355 nm) in the presence of ODN-G1 (○), -G2 (●), and -G3 (△) vs concentration of ODN.

Sequence Dependence of the One-Electron Oxidation of ODN by ^{3}NIP*. Under the condition where the NI derivatives (NIN and NIO) associate with ODN, it is difficult to distinguish the contributions of the free NI and associated NI to the one-electron oxidation of ODN. Although NIP in the ground state does not associate with ODN because of the electrostatic repulsion of the negatively charged phosphate ions with the negatively charged ODN backbone as described above, collision between NIP in the triplet excited state and ODN results in the charge separation. Therefore, we examined the sequence dependence on the one-electron oxidation of ODN by ^{3}NIP* during the LFP of ODN.

The formation yield of NIP$^{\bullet-}$ indicated by the optical density at 400 nm (ΔOD_{400}) during the 355-nm LFP in the presence of ODN is shown in Figure 4. The yield of NIP$^{\bullet-}$ (ΔOD_{400}) increased with the increasing concentration of ODN, indicating that the one-electron oxidation of ODN by ^{3}NIP* occurred. The efficiency of the one-electron oxidation of ODN by ^{3}NIP* increased in the order G1 < G2 < G3. The ratio of 1:1.9:2.8 for the efficiency of the one-electron oxidation of ODN-G1, -G2, and -G3 was obtained from the slopes of the linear plots shown in Figure 4. This order is in good agreement with the previous results observed in the photosensitized oxidation of ODN on the basis of PAGE and electrochemical experi-

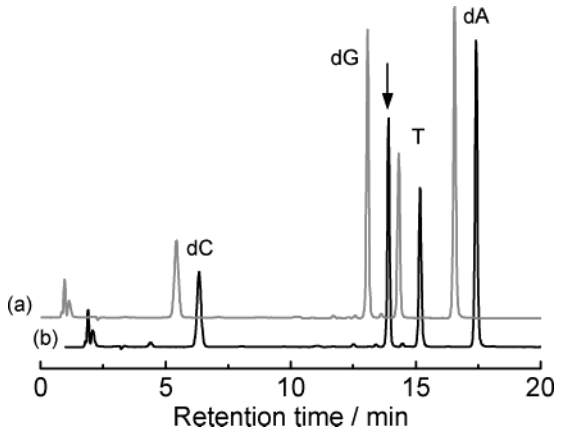

Figure 5. HPLC analysis before (a) and after (b) irradiation of a mixture of ODN-G3 and NIN for 10 min and enzymatic digestion. A reaction mixture containing 40 μM ODN and 100 μM NIN in sodium phosphate buffer (pH = 7.0) was irradiated with a high-pressure Hg lamp fitted with a 330 nm filter.

ments.[10,19,20] In the studies using sequencing gels, the selectivity for oxidation of the 5′-G of GG doublets was observed upon irradiation in the presence of photosensitizers followed by the piperidine treatment of labeled oligonucleotides with one-electron oxidants. For instance, Hickerson et al. recently reported that oxidative cleavage of DNA containing G, GG, and GGG occurred with a cleavage ratio of 1.0:3.7:5.3, respectively.[20] In a series of mechanistic studies of the sequence selectivity of DNA oxidation, Saito and Sugiyama demonstrated that the stacking effect of consecutive G bases decreased the ionization potential on the basis of the high-level ab initio molecular orbital calculations of DNA.[5,21] Thorp et al. showed that the rate of oxidation of the 5′-G in a GG doublet was enhanced by a factor of 12 compared to the isolated G on the basis of the electrochemical experiments.[19] Kinetic studies using transient absorption measurements were reported by Lewis et al.[10] They determined the equilibrium constants from monitoring the hole transport between G and GG and between G and GGG and demonstrated the difference in thermodynamic stability (ΔG) of consecutive G's; the ΔG values of GG and GGG versus G are -0.052 and -0.077 eV, respectively. Our results of the charge-separation yield between ^{3}NIP* and ODNs containing G, GG, and GGG are similar to their results, confirming that the ionization potential of G is lowered by the stacking interaction between G's.

Comparison of the Transient Absorption Measurement with HPLC Analysis. In an effort to clarify the relationship between the LFP studies of the transient intermediates and the actual amount of the ODN oxidative lesion, we quantified the consumption of G in the photosensitized one-electron oxidation of ODN using reverse-phase HPLC analysis.[1] Solutions containing NI derivatives and ODN were irradiated with a high-pressure mercury lamp fitted with a 330-nm cutoff filter under the aerated condition at 4 °C. The reaction mixture was then directly subjected to enzymatic digestion.

The selective consumption of G was observed for all three NI derivatives as shown in Figure 5, indicating that the reaction leading to the decomposition of G was due to the electron transfer from G to the NI derivatives in the excited state. Furthermore, we confirmed the oxidative G lesion of ODN by monitoring the formation of imidazolone, which is one of the oxidative products.[22] Consumption of G increased in the order ODN-G1 < ODN-G2 < ODN-G3 (Table 2). These results of the HPLC analysis are similar to that of the LFP of solutions

TABLE 2: Consumption of G in the Photooxidation of ODN by NI Derivatives

	consumption of G (%)		
NI derivatives	ODN-G1	ODN-G2	ODN-G3
NIP	0.8	2.4	4.3
NIO	1.3	9.1	12
NIN	0.5	4.5	7.5

SCHEME 4: Kinetic Schemes of the One-Electron Oxidation of ODN via (a) ^{1}NIN* and (b) ^{3}NIP* in the Presence of O_2[a]

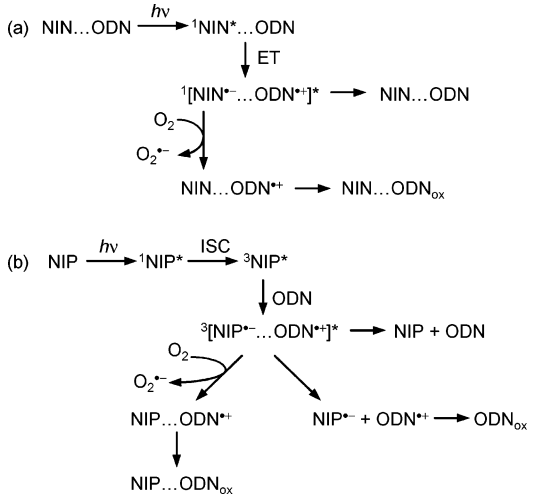

[a] $ODN^{\bullet+}$ reacts with H_2O or O_2 or both to give ODN_{ox} as the product.

containing NIP, suggesting that the charge-separation efficiency on the diffusion process is related to the actual oxidative lesion of ODN. However, the oxidative lesion of ODN was similarly observed for NIN the radical anion of which was not observed in the LFP experiments because of the rapid charge separation between ^{1}NI* and the adjacent nucleobase and recombination between $NI^{\bullet-}$ and adjacent nucleobase radical cation.

This difference would be attributed to the presence of O_2 in the HPLC analysis. Namely, an electron on $NIN^{\bullet-}$ generated from the electron transfer from the adjacent nucleobase to ^{1}NIN* was removed by O_2 to give $O_2^{\bullet-}$ in the aqueous solution. To examine the effect of O_2 on the oxidative process, we carried out HPLC analysis under the condition where the sample was purged with Ar but could not investigate the photoreaction because the photosensitizer NIN decomposed faster than the consumption of G. These results indicate that electron removal from $NI^{\bullet-}$ generated via the charge-separation process by O_2 can reproduce NI and reaction of $G^{\bullet+}$ with O_2 plays an important role to induce the oxidative lesion in DNA. Recycling of the photosensitizer in the presence of O_2 has been previously reported.[1,8,23]

Importance of O_2 and Its Concentration on the One-Electron Oxidative DNA Damage. The discrepancy between the results of the LFP and HPLC experiments implies the importance of O_2 involved in the photochemical DNA oxidation. The kinetic schemes of the one-electron oxidation of ODN involving O_2 are shown in Scheme 4. In the case of NIN (Scheme 4a), the one-electron oxidation of ODN proceeds with ^{1}NIN* in the ground-state complex between NIN and ODN, resulting in the formation of the singlet radical ion pair of $^1[NIN^{\bullet-}/ODN^{\bullet+}]$*, and then charge recombination rapidly occurs to recover the complex in the absence of O_2. However, in the presence of O_2, $^1[NIN^{\bullet-}/ODN^{\bullet+}]$* can react with O_2 to yield $O_2^{\bullet-}$ and a hole in ODN, leading to the DNA oxidative damage.

In contrast, in the case of NIP (Scheme 4b), the one-electron oxidation of ODN proceeds with ^{3}NIP* because of no ground-state complex between NIP and ODN, resulting in the formation of the triplet radical ion pair of ^{3}[NIP$^{\bullet-}$/ODN$^{\bullet+}$]* and then partial dissociation to free NIP$^{\bullet-}$ and ODN$^{\bullet+}$ by solvent separation. Therefore, ^{3}NIP* can also produce a DNA lesion in the absence of O_2. In the presence of O_2, ^{3}[NIP$^{\bullet-}$/ODN$^{\bullet+}$]* and free NIP$^{\bullet-}$ can be quenched. Accordingly, the concentration of O_2 in the solution might determine which processes play an important role in the effective DNA oxidation.

However, considering that the O_2 concentration is very low in the cell nucleus,[24] the results obtained from the LFP experiments may indicate the actual DNA oxidative process. Effective G decomposition seems to be difficult under a low O_2 concentration unless the charge-separation state between the photosensitizer and G has a long lifetime. Accordingly, it is suggested that the effective photooxidation of ODN occurs with a photosensitizer in the triplet excited state rather than in the singlet excited state because the lifetime of the triplet charge-separation state becomes much longer because of the spin-forbidden charge recombination between the photosensitizer radical anion and nucleobase radical cation in the triplet radical ion pair. Therefore, the formation of photosensitizers in the triplet excited state plays an important role in the actual oxidative DNA damage.[1]

Conclusions

The photochemical mechanism of the NI-photosensitized one-electron oxidation of ODN was investigated by monitoring the transient absorptions of ^{3}NI* and NI$^{\bullet-}$ during the nansecond LFP. With respect to the effects of the binding of NI to ODN, the formation yield of the ^{3}NI* derivatives immediately after the 355-nm laser flash decreased with an increase in K of the NI derivatives because of the singlet electron-transfer pathway. By monitoring the transient absorption of NIP$^{\bullet-}$ produced by electron transfer from ODN to ^{3}NIP*, it was found that the charge-separation efficiency increased for the sequence of sequential G's because of the oxidation potential of G lowered by the stacking effect of the G's. Furthermore, the correlation between the NI derivatives in the excited state and oxidative lesion was investigated by HPLC analysis, suggesting that the presence of O_2 in the solution was crucial to the photooxidation mechanism of DNA. Considering the low concentration of intracellular O_2, generation of the photosensitizer in the triplet state may be crucial to the actual DNA oxidative lesion because the charge-separation state in the triplet excited state has a longer lifetime compared with that in the singlet excited state.

Acknowledgment. This work has been partly supported by a Grant-in-Aid for Scientific Research from Ministry of Education, Science, Sport and Culture of Japan.

References and Notes

(1) Armitage, B. *Chem. Rev.* **1998**, *98*, 1171−1200.

(2) (a) Burrows, C. J.; Muller, J. G. *Chem. Rev.* **1998**, *98*, 1109−1151. (b) Steenken, S. *Chem. Rev.* **1989**, *89*, 503−520.

(3) Steenken, S.; Jovanovic, S. V. *J. Am. Chem. Soc.* **1997**, *119*, 617−618.

(4) Seidel, C. A. M.; Schulz, A.; Sauer, M. H. M. *J. Phys. Chem.* **1996**, *100*, 5541−5553.

(5) Sugiyama, H.; Saito, I. *J. Am. Chem. Soc.* **1996**, *118*, 7063−7068.

(6) Rogers, J. E.; Weiss, S. J.; Kelly, L. A. *J. Am. Chem. Soc.* **2000**, *122*, 427−436.

(7) (a) Rogers, J. E.; Le, T. P.; Kelly, L. A. *Photochem. Photobiol.* **2001**, *73*, 223−229. (b) Candeias, L. P.; Steenken, S. *J. Am. Chem. Soc.* **1993**, *115*, 2437−2440. (c) Brun, A. M.; Harriman, A. *J. Am. Chem. Soc.* **1991**, *113*, 8153−8159. (d) Saito, I.; Takayama, M.; Sugiyama, H.; Nakatani, K.; Tsuchida, A.; Yamamoto, M. *J. Am. Chem. Soc.* **1995**, *117*, 6406−6407.

(8) Armitage, B.; Yu, C. J.; Devadoss, C.; Schuster, G. B. *J. Am. Chem. Soc.* **1994**, *116*, 9847−9859.

(9) (a) Kawai, K.; Wata, Y.; Hara, M.; Tojo, S.; Majima, T. *J. Am. Chem. Soc.* **2002**, *124*, 3586−3590. (b) Kawai, K.; Wata, Y.; Ichinose, N.; Majima, T. *Angew. Chem., Int. Ed.* **2000**, *39*, 4327−4329.

(10) Lewis, F. D.; Liu, X. Y.; Liu, J. Q.; Hayes, R. T.; Wasielewski, M. R. *J. Am. Chem. Soc.* **2000**, *122*, 12037−12038.

(11) Ma, J. H.; Lin, W. Z.; Wang, W. F.; Han, Z. H.; Yao, S. D.; Lin, N. Y. *J. Photochem. Photobiol., B* **2000**, *57*, 76−81.

(12) (a) Rajski, S. R.; Barton, J. K. *Biochemistry* **2001**, *40*, 5556−5564. (b) Nunez, M. E.; Hall, D. B.; Barton, J. K. *Chem. Biol.* **1999**, *6*, 85−97. (c) Hall, D. B.; Kelley, S. O.; Barton, J. K. *Biochemistry* **1998**, *37*, 15933−15940. (d) Barton, J. K. *Pure Appl. Chem.* **1998**, *70*, 873−879. Kawai, K.; Takada, T.; Tojo, S.; Majima, T. *Tetrahedron Lett.* **2002**, *43*, 89−91. (e) Kawai, K.; Takada, T.; Tojo, S.; Majima, T. *Tetrahedron Lett.* **2002**, *43*, 8083−8085. (f) Kawai, K.; Takada, T.; Tojo, S.; Ichinose, N.; Majima, T. *J. Am. Chem. Soc.* **2001**, *123*, 12688−12689.

(13) Rogers, J. E.; Kelly, L. A. *J. Am. Chem. Soc.* **1999**, *121*, 3854−3861.

(14) (a) Aveline, B. M.; Matsugo, S.; Redmond, R. W. *J. Am. Chem. Soc.* **1997**, *119*, 11785−11795. (b) Saito, I.; Takayama, M.; Sugiyama, H.; Nakatani, K. *J. Am. Chem. Soc.* **1995**, *117*, 6406−6407.

(15) Oza, V. B.; Corcoran, R. C. *J. Org. Chem.* **1995**, *60*, 3680−3684.

(16) McGhee, J. D.; Von Hippel, P. H. *J. Mol. Biol.* **1974**, *86*, 469−489.

(17) Yen, S. F.; Gabbay, E. J.; Wilson, W. D. *Biochemistry* **1982**, *21*, 2070−2076.

(18) (a) SantaLucia, J. J. *Proc. Natl. Acad. Sci. U.S.A.* **1998**, *95*, 1460−1465. (b) Allawi, H. T.; Santa Lucia, J., Jr. *Biochemistry* **1997**, *36*, 10581−10594.

(19) Sistare, M. F.; Codden, S. J.; Heimlich, G.; Thorp, H. H. *J. Am. Chem. Soc.* **2000**, *122*, 4742−4749.

(20) Hickerson, R. P.; Prat, F.; Muller, J. G.; Foote, C. S.; Burrows, C. J. *J. Am. Chem. Soc.* **1999**, *121*, 9423−9428.

(21) Saito, I.; Nakamura, T.; Nakatani, K.; Yoshioka, Y.; Yamaguchi, K.; Sugiyama, H. *J. Am. Chem. Soc.* **1998**, *120*, 12686−12687.

(22) (a) Angelov, D.; Spassky, A.; Berger, M.; Cadet, J. *J. Am. Chem. Soc.* **1997**, *119*, 11373−11380. (b) Cadet, J.; Berger, M.; Buchko, G. W.; Joshi, P. C.; Raoul, S.; Ravanat, J. L. *J. Am. Chem. Soc.* **1994**, *116*, 7403−7404.

(23) Ly, D.; Kan, Y.; Armitage, B.; Schuster, G. B. *J. Am. Chem. Soc.* **1996**, *118*, 8747−8748.

(24) (a) Dussy, A.; Meggers, E.; Giese, B. *J. Am. Chem. Soc.* **1998**, *120*, 7399−7403. (b) Zander, R. *Oxygen Transport to Tissue II. Proceedings of the Second International Symposium, Mainz, March 12−14, 1975*.